



LJMU Research Online

Hambrecht, L, Brown, RP, Piel, AK and Wich, SA

Detecting 'poachers' with drones: Factors influencing the probability of detection with TIR and RGB imaging in miombo woodlands, Tanzania

<http://researchonline.ljmu.ac.uk/id/eprint/10327/>

Article

Citation (please note it is advisable to refer to the publisher's version if you intend to cite from this work)

Hambrecht, L, Brown, RP, Piel, AK and Wich, SA (2019) Detecting 'poachers' with drones: Factors influencing the probability of detection with TIR and RGB imaging in miombo woodlands, Tanzania. *Biological Conservation*. 233. pp. 109-117. ISSN 0006-3207

LJMU has developed [LJMU Research Online](#) for users to access the research output of the University more effectively. Copyright © and Moral Rights for the papers on this site are retained by the individual authors and/or other copyright owners. Users may download and/or print one copy of any article(s) in LJMU Research Online to facilitate their private study or for non-commercial research. You may not engage in further distribution of the material or use it for any profit-making activities or any commercial gain.

The version presented here may differ from the published version or from the version of the record. Please see the repository URL above for details on accessing the published version and note that access may require a subscription.

For more information please contact researchonline@ljmu.ac.uk

<http://researchonline.ljmu.ac.uk/>

Manuscript Details

Manuscript number	BIOC_2018_1492
Title	Detecting 'poachers' with drones: Factors influencing the probability of detection with TIR and RGB imaging in miombo woodlands, Tanzania
Article type	Full Length Article

Abstract

Conservationists increasingly employ drones to reduce poaching of animals. However, there are no published studies on the detection probability of poachers and the factors influencing detection. In an experimental setting with voluntary subjects, we evaluated the influence of various factors on poacher detection probability: camera (visual spectrum: RGB and thermal infrared: TIR), density of canopy cover, subject distance from the image centreline, subject contrast against the background, altitude of the drone and image analyst. We manually analysed the footage and marked all recorded subject detections. A multilevel model statistical approach was used to analyse the TIR image data and a general linear model approach was used for the RGB image data. We found that the TIR camera had a higher detection probability than the RGB camera. Detection probability in TIR images was significantly influenced by canopy density, subject distance from the centreline and the analyst. Detection probability in RGB images was significantly influenced by canopy density, subject contrast against the background, altitude and the analyst. Overall, our findings indicate that TIR cameras improve human detection, particularly at cooler times of the day, but this is significantly hampered by thick vegetation cover. The effects of diminished detection with increased distance from the image centreline can be improved by increasing the overlap between images although this requires more flights over a specific area. Analyst experience also contributed to detection probability, but this might cease to become a problem following the development of automated detection using machine learning.

Keywords	uav; poaching, thermal; comparison; distance; contrast
Taxonomy	Wildlife Conservation, Environmental Protection, Environmental Monitoring, Environmental Technology, Environmental Issues of Natural Resources
Corresponding Author	Leonard Hambrecht
Corresponding Author's Institution	Liverpool John Moores University
Order of Authors	Leonard Hambrecht, RP Brown, Alex Piel, Serge Wich

Submission Files Included in this PDF

File Name [File Type]

hambrecht_cover_page_october18.docx [Cover Letter]

hambrecht_title_page_october18.docx [Title Page (with Author Details)]

hambrecht_new_submission_blinded_manuscript_october18.docx [Manuscript (without Author Details)]

To view all the submission files, including those not included in the PDF, click on the manuscript title on your EVISE Homepage, then click 'Download zip file'.

Detecting ‘poachers’ with drones: Factors influencing the probability of detection with TIR and RGB imaging in miombo woodlands, Tanzania

by

Leonard Hambrecht ^{1*}, Richard P. Brown ¹, Alex K. Piel ¹, and Serge A. Wich ^{1,2}

¹ School of Natural Sciences and Psychology, Liverpool John Moores University, UK

² Institute for Biodiversity and Ecosystem Dynamics, University of Amsterdam, Amsterdam, The Netherlands

* Corresponding author. Email: lennyhambrecht@pm.me
Address: Haydnstrasse 42, 40593 Düsseldorf, Germany

New Submission to
Biological Conservation
Special Issue
Conservation Drones

October 2018



Authors statements

We the undersigned declare that this manuscript is **original**, has not been published before and is not currently being considered for publication elsewhere.

We wish to confirm that there are **no known conflicts of interest** associated with this publication and there has been no significant financial support for this work that could have influenced its outcome.

We confirm that the manuscript has been read and **approved by all named authors** and that there are no other persons who satisfied the criteria for authorship but are not listed. We further confirm that the order of authors listed in the manuscript has been approved by all of us.

We confirm that we have given due consideration to the **protection of intellectual property** associated with this work and that there are no impediments to publication, including the timing of publication, with respect to intellectual property. In so doing we confirm that we have followed the regulations of our institutions concerning intellectual property.

We further confirm that any aspect of the work covered in this manuscript that has involved either experimental animals or human patients has been conducted with the **ethical approval** of all relevant bodies and that such approvals are acknowledged within the manuscript.

We understand that the **Corresponding Author** is the sole contact for the Editorial process (including Editorial Manager and direct communications with the office). He/she is responsible for communicating with the other authors about progress, submissions of revisions and final approval of proofs. We confirm that we have provided a current, correct email address which is accessible by the Corresponding Author.

We confirm that this paper in any form has **not been previously been submitted** in Biological Conservation Journal.

This research was conducted as dissertation by Leonard Hambrecht for the course “M.Sc. Wildlife Conservation & UAV Technology” 2016/2017 at the Liverpool John Moores University.

Main Findings

The study focused on the comparison between TIR (thermal infrared) cameras and RGB (visual spectrum) cameras attached to a drone for detecting poachers in miombo woodlands in Tanzania. We found that TIR cameras improve detection of poachers over RGB cameras particular in cooler times of the day. However, detection is significantly hampered by thick vegetation cover. The effects of diminished detection with increased distance from the image centreline can be improved by increasing the overlap between images although this requires more flights over a specific area. Analysts experience can furthermore improve the probability of detection. These finding can help drone operators to evaluate the limitations of drones for detecting poachers and to ultimately increase the drone defectiveness.

Authors Signatures

26/10/2018
Date, Leonard Hambrecht



28/10/18
Date, Richard P. Brown



26/10/2018
Date, Alex K. Piel



26/10/2018
Date, Serge A. Wich



Detecting ‘poachers’ with drones: Factors influencing the probability of detection with TIR and RGB imaging in miombo woodlands, Tanzania

Leonard Hambrecht ^{1*}, Richard P. Brown ¹, Alex K. Piel ¹, and Serge A. Wich ^{1,2}

¹ School of Natural Sciences and Psychology, Liverpool John Moores University, UK

² Institute for Biodiversity and Ecosystem Dynamics, University of Amsterdam, Amsterdam, The Netherlands

* Corresponding author. Email: lennyhambrecht@pm.me

Address: Haydnstrasse 42, 40593 Düsseldorf, Germany

Acknowledgements

The use of human test subjects for this research was approved by the “University Research Ethics Committee” (UREC) of LJMU, with an approval reference of 17/NSP/008. Flights were performed according to the “LJMU Operations Manual for UAV’s” as well as the “Aeronautical Information Circular” (AIC) number 5/17 (Pink 62) of 1 January 2017 and according to the “Tanzania Civil Aviation Regulations” (TCARs).

LH specially thanks Dr. Thomas Grussenmeyer and Charlotte Jense for their time analysing the drone footage and Stefan Thamke from the TeAx Technology company also deserves credit for his support. SW thanks WWF Netherlands for financial support and thanks goes to Tascha Dean, Molly Frost, and John Lamb for proofreading the script. Furthermore, we would like to thank Andy Goodwin and Ian Thomson for support for the drone. Special thanks also go to the students of the 2016/2017 M.Sc. course Wildlife Conservation & UAV Technology as well as to the GMERC (formerly Ugalla Primate Project) staff for their support and patience. The authors would also like to thank: Claire Rigby, Finnoula Taylor, Megan Melia, Josph Goode, Derek Dwane, Naomi Jones, Rory Andrews, Anna Starkey, Joseph Phillips, Naomi Davies, Molly Frost, Evie Hyland, Olivia Evans, Jade Musto, Andy Tomlinson, Glory Marie, Mashaka Alimasi, Godfrey Stephano, Mlela Juma, Hussein Juma, Baruana Juma, Abdallah Said, Roda Dominick and Milka Hyamubi. Finally, thanks to Dr. Bryan Pijanowski of Purdue University for the video footage of the data collection.

Declaration of Interest

We wish to confirm that there are no known conflicts of interest associated with this publication and there has been no significant financial support for this work that could have influenced its outcome.

1 **Detecting ‘poachers’ with drones: Factors influencing the probability of**
2 **detection with TIR and RGB imaging in miombo woodlands, Tanzania**

3
4 **Abstract**

5 Conservationist increasingly employ drones to reduce poaching of animals. However, there are no
6 published studies on the detection probability of poachers and the factors influencing detection. In
7 an experimental setting with voluntary subjects, we evaluated the influence of various factors on
8 poacher detection probability: camera (visual spectrum: RGB and thermal infrared: TIR), density of
9 canopy cover, subject distance from the image centreline, subject contrast against the background,
10 altitude of the drone and image analyst. We manually analysed the footage and marked all recorded
11 subject detections. A multilevel model statistical approach was used to analyse the TIR image data
12 and a general linear model approach was used for the RGB image data. We found that the TIR
13 camera had a higher detection probability than the RGB camera. Detection probability in TIR
14 images was significantly influenced by canopy density, subject distance from the centreline and the
15 analyst. Detection probability in RGB images was significantly influenced by canopy density,
16 subject contrast against the background, altitude and the analyst. Overall, our findings indicate that
17 TIR cameras improve human detection, particularly at cooler times of the day, but this is
18 significantly hampered by thick vegetation cover. The effects of diminished detection with
19 increased distance from the image centreline can be improved by increasing the overlap between
20 images although this requires more flights over a specific area. Analyst experience also contributed
21 to detection probability, but this might cease to become a problem following the development of
22 automated detection using machine learning.

23
24
25
26
27
28
29
30
31
32
33
34
35
36 **Keywords:**

37 UAV, drone, thermal, TIR, RGB, comparison, contrast, distance, centerline, poachers, people, time
38 of day, poaching, conservation, canopy, density

39 **1 Introduction**

40 Poaching, the unlawful harvest of wildlife products, supports illegal global wildlife trade and is a
41 major conservation issue due to its impact on species extinctions. The demand for illegal wildlife
42 products has risen in the few last years with 7000 species recorded as having been trafficked
43 (Lawson and Vines, 2014; United Nations Office on Drugs and Crime, 2016). This results in the
44 decline of threatened species, as well as rise in international security threats and economic losses
45 (Balazs, 2016; Becker et al., 2013; Chapron et al., 2008; Liberg et al., 2012; Naidoo et al., 2016;
46 United Nations Office on Drugs and Crime, 2016). Wildlife enforcement officers and
47 conservationists try to fight poaching using a variety of methods, such as reducing demand in key
48 areas such as Asia, implementing community conservation areas, deploying ranger patrols in
49 protected areas, strengthening wildlife laws, dehorning rhinos and implementing new technologies
50 such as DNA mapping, mobile biological sensors and drones (Dinerstein et al., 2017; Lunstrum,
51 2014; Mukwazvure and Magadza, 2014). Drones are a cost-effective and flexible tool that can be
52 used in the field to monitor protected habitat and gather intelligence on wildlife crime activities
53 (Koh and Wich, 2012; Linchant et al., 2015; World Bank, 2018). This intelligence includes the
54 detection of poachers in the field (Air Shepherd, 2017; Mulero-Pázmány et al., 2014; Smart parks,
55 2018).

56 There are several key safety, technical and practical differences between the use of drones for
57 detecting poachers and the more traditional use of manned aircrafts. Most importantly, the latter
58 pose a higher risk to the operator as poachers can deploy powerful weapons. In contrast, drones
59 allow detection while simultaneously minimizing confrontations with poachers (Baggaley, 2017;
60 Parveen, 2016). Secondly, manned aircraft require an on-board observer, while drones can use a
61 variety of sensors to record still and moving images that either need to be viewed as a live stream or
62 analysed after the flight. Additional advantages of using drones include their cost-effectiveness, the
63 fact that they do not require a runway and that they can be programmed to follow precisely a
64 predefined path (Kakaes et al., 2015). Furthermore, drones have been found to be able deliver more
65 accurate animal count data than traditional ground-based surveys (Hodgson et al., 2018).

66 Although their deployments in anti-poaching efforts are promising, there are no studies that have
67 explicitly investigated the factors that determine detection probability in this specific context.
68 However, it is important to do so for several reasons, including the optimization of flight patterns to
69 improve detection and identify the environmental conditions under which poachers are likely to be
70 missed during drone missions. Fixed wing drones are the preferred tool for anti-poaching operations
71 because of their long flight duration and extended range (Mulero-Pázmány et al., 2014; Olivares-
72 Mendez et al., 2015).

73 There are various factors that affect the probability of detecting animals – and potentially humans –
74 including body size, position of the sun, distance from the transect, group density, target contrast,
75 terrain ruggedness, animal activity, vegetation type and camera type (Caughley et al., 1976;
76 Chrétien et al., 2015; Chrétien et al., 2016; Patterson et al., 2015; Ransom, 2012; Schlossberg et al.,
77 2016; Zabransky et al., 2016). Two types of camera are most typically used: those that use the Red
78 Green Blue colour model (RGB) and thermal infrared (TIR) devices. RGB cameras acquire images
79 in the light spectrum visible to humans and can be found on most consumer drones. They are often
80 more affordable and may have a higher resolution than TIR cameras (Wich and Koh, 2018). TIR
81 cameras capture infrared radiation which is emitted as heat from different sources of energy as well
82 as endothermic organisms (Vollmer and Möllmann, 2010). This makes them useful for detecting
83 poachers who generally operate at night to reduce the risk of detection (Mulero-Pázmány et al.,
84 2014). TIR cameras have been used for decades to remotely sense wildlife and, with drones, the
85 focus has been to survey large terrestrial as well as marine mammals (Chrétien et al., 2016, 2015;
86 Christiansen et al., 2014; Seymour et al., 2017; Wride and Baker, 1977). In recent years, algorithms
87 have been developed to improve the detection of animals in TIR camera footage and made
88 automatic detection possible (Burke et al., 2018a, 2018b; Christiansen et al., 2014; Longmore et al.,
89 2017; Seymour et al., 2017). There are no studies that have examined the detection probabilities of
90 poachers by RGB and TIR imaging cameras.

91 In this study we investigate the factors that determine the detection probability of people (subjects)
92 in a Miombo woodland in Tanzania. We conducted an experiment in which a drone with RGB and
93 TIR imaging cameras was flown over a group of test subjects to determine which of the following
94 variables influenced detection probability: camera type (RGB or TIR), canopy cover, subjects
95 distance from image centreline, contrast between subject and background and the altitude of the
96 drone. Contrasts between subjects and the background was controlled through use of differently
97 coloured t-shirts. We hypothesized that the probability of detection is negatively affected by a dense
98 canopy cover, a larger distance from the image centreline and higher altitude for both RGB and TIR
99 cameras. In addition, we hypothesized that a larger contrast between the subject and background
100 increases the probability of detection for RGB cameras and that detection will be better with the
101 TIR camera during low light conditions.

102 **2 Methods**

103

104 **2.1. Study Area**

105 The study was conducted at the Issa study site (-5.50, 30.56) in the western part of Tanzania. This
106 location lies at 1500 meters (m) above sea level and the dominant vegetation type is miombo
107 woodland (dominated by the genera: *Brachystegia* and *Julbernardia*) (Piel et al., 2015). The data
108 were collected in March 2017, which coincides with the end of the rainy season, when the
109 vegetation is green and dense across the region.

110

111 **2.2. Drone and Cameras**

112 We used a multicopter consisting of a DJI F550 frame with a Pixhawk flight controller. The drone
113 carried two cameras: 1) a 16 MP RGB Survey 2 camera (Mapir, 2016a) with a field of view (FOV)
114 of 82° which was triggered by the flight controller to take an image at 10m intervals, 2) a
115 ThermalCapture v1.0 TIR camera with a TAU 640 core with a FOV of 45° (TeAx Technology,
116 2018). The RGB camera was set at ISO 100 and a shutter speed of 1/250. The TIR camera
117 continuously recorded video with automatic settings. All flights were conducted by one of the
118 authors (SW). The two cameras used were: 1) a 16 MP RGB Survey 2 camera (Mapir, 2016a) with
119 a field of view (FOV) of 82° which was triggered by the flight controller to take an image at an
120 interval of every 10 m, 2) a ThermalCapture v1.0 TIR camera with a TAU 640 core with a FOV of
121 45° (TeAx Technology, 2018). The RGB camera was set at ISO 100 and a shutter speed of 1/250.
122 The TIR camera continuously recorded video with automatic settings.

123

124 **2.3. Flight Path**

125 Drone flight paths (Appendix A.1) were created using Mission Planner software (ArduPilot Dev
126 Team, 2017) and uploaded to the Pixhawk flight controller. Take-offs and landings were conducted
127 in loiter mode whereas auto mode was used for the flight pattern. The flight pattern consists of three
128 parallel rows with a length of 70 m each and a connection section of 30 m in length between each
129 row. The descent (dotted line) leads the drone back to its take-off location (Appendix A, Black
130 Square). The flight pattern was performed twice at two different altitudes (70 m and 100 m),
131 providing six rows per flight. The upper altitude of 100 m was chosen as it was close to the usual
132 operation altitude of fixed wing drones while still staying within the legal boundaries of 122 m (400
133 ft.) (Tanzania Civil Aviation Authority, 2017). The lower altitude of 70 m was chosen as the lowest
134 recommended altitude for safe operation of fixed wing drones and the 70 – 100 m range was
135 considered suitable for this type of drone. The average flight duration during the data collection was

136 approximately six minutes at a ground speed of 4 – 5 m/s. Two flight areas were set up at different
137 locations with the same flight pattern as can be seen in Appendix A. A total of seven flights were
138 conducted: four in flight area 1 and three in flight area 2. A dawn flight (7:30 am) was conducted in
139 each area, followed by a second flight at dusk on the same day (7:00 pm). These times were chosen
140 to improve the image quality of the TIR images, as lower environmental temperatures create a
141 greater contrast between a person and their surroundings. However, low light levels during several
142 of these flights meant that the RGB camera was unable to produce sufficiently exposed images.

143

144 **2.4. Location**

145 We selected 24 locations within each flight area and then randomly assigned each test subject to one
146 of them. The locations were chosen on-site to create an equal spatial distribution of locations in the
147 area and with equal frequencies of dense and less dense canopy covers. GPS coordinates of the
148 locations were recorded with the MobileMapper 20 (MM20) model by Spectra Precision. The
149 MM20 has an accuracy of <2 m in real-time (Trimb et al., 2013).

150

151 **2.5. Test Subjects and T-shirt Colours**

152 A group of 10 - 20 voluntary subjects (varying per flight) were positioned within the flight area for
153 each of the flights. Each subject wore a standard red, green or blue t-shirt to create a controlled
154 contrast with the background. Each subject wore the same t-shirt and was positioned at the same
155 location for each flight. The test subjects were required to stay at their assigned locations during the
156 flights, with a single subject assigned to each location.

157

158 **2.6. Canopy Cover**

159 The canopy densities of the locations were measured by photographing the canopy and calculating
160 the canopy density in the software CanopyDigi (Goodenough and Goodenough, 2016). CanopyDigi
161 gives a calculated value between 0 (open sky) and 1 (completely covered) for each image. Photos
162 were taken with a 24-mm fixed focal length lens mounted on an APS-C camera body with a 1.6
163 crop sensor resulting in a FOV of 59°. The camera was set up on a tripod at a height of 1.5 m and
164 aligned horizontally using a level. Goodenough and Goodenough (2012) recommend a cloudy sky
165 for best results when photographing the canopy cover. However, this was not always possible and
166 most images were taken with a clear sky and the sun in the frame. This resulted in brighter images
167 which were compensated by adjusting the auto exposure of the camera by -1 stop. This adjustment
168 darkened the images to compensate for the bright sky. The camera was manually focused on the

169 closest branch to ensure sharp images and an aperture of f/16 was used for a sufficient depth of
170 field. ReaConverter Light (ReaSoft Development, 2017) was used to convert the images into the file
171 format required by CanopyDigi (Goodenough and Goodenough, 2012). The threshold values in
172 CanopyDigi were adjusted to deal with images in which the sun was visible in the frame. The
173 thresholds used a range from 45 to 125.

174

175 **2.7. Image Processing and analyses**

176 Footage from the two cameras were checked for quality. Any footage taken during take-off, landing
177 or from the connection and transition piece was discarded. We reviewed the footage from the TIR
178 camera in the proprietary ThermoViewer 2.1.2 software (TeAx Technology, 2017). The Non
179 Uniformity Correction (NUC) option was turned on in ThermoViewer, as recommended by the
180 manufacturers. Video footage was converted into 3 to 4 JPG images per row. We converted the
181 RGB camera footage from raw into JPG images using the MAPIR plugin (Mapir, 2016b) for the
182 Fiji software (Schindelin et al., 2012). RGB images were then downscaled to the same resolution as
183 the TIR images (701x512) with the Exiftool software (Harvey, 2017). This allows for a universal
184 comparison of the two image types, independent of resolution quality.

185 Images were analysed separately by three independent analysts, none of whom had previous
186 experience in detecting human subjects in aerial images. Images were provided to the analysts in a
187 random order. In avoiding the sequential showing of all images from one row, analysts could not
188 apply their knowledge of locations from previous images to detect the subjects. The plugin in Cell
189 Count (De Vos, 2010) for the ImageJ .1.8.0 software (Rueden et al., 2017) was used to annotate
190 detected subjects in the images.

191 The images were not georeferenced and the subjects are identified by their relative location to each
192 other and to landmarks, and the colour of their t-shirts (Appendix B). The results of images from the
193 same row were summarized, thereby simulating a tracking motion in moving images. The multiple
194 angles simulate a tracking motion of a subject in the frame. The tracking enhances the probability of
195 detection because of the multiple camera angles (Gonzalez et al., 2016).

196

197 **2.8. Calculating the Distance to the Centreline of the Image**

198 We calculated the distance from each subject to the centreline using QGIS 2.18 (Quantum GIS
199 Development Team, 2017). The calculation of the distances used the GPX track as centreline and
200 the shortest distance to each location was calculated with the distance matrix tool.

201

202 2.9. Statistical Analysis

203 All analyses were carried out using the lme4, glm2 and MuMIn packages in R v3.4.1 (Bates et al.,
 204 2017; R Core Team, 2017). We chose a multilevel model approach to accomodate random effects,
 205 repeated measurements and crossed data (Field et al., 2012; Grueber et al., 2011; Qian et al., 2010).
 206 Following the approach suggested by Grueber et al. (2011), entries with missing data were excluded
 207 from the analysis. We used a general linear model for the data from the RGB camera as described
 208 below. All responses were binary (detection (1)/no-detection (0)) and thus a logit link function was
 209 used for all analyses. The variables used in the code for the global data models can be seen in Table
 210 1.

211 *Table 1 Overview of the tested variables with description.*

No	Variable type		Variable	Definition
<u>Response variable</u>				
0	Binomial		Detected	Detected = 1; undetected = 0
<u>Predictor variable</u>				
1	Continuous	Fixed	<i>Canopy density</i>	Canopy density between 0 and 1
2	Continuous	Fixed	<i>Distance</i>	Distance from centreline (m)
3	Binomial	Fixed	<i>Altitude</i>	70 m = 0; 100 m = 1
4	Nominal	Fixed	<i>Colour</i>	White/ TIR = 0; red = 1; blue = 2; green = 3
5	Binomial	Fixed	<i>Time of day</i>	Dusk = 0; dawn = 1
6	Nominal	Fixed	<i>Analyst</i>	Analyst 1, 2, 3
<u>Hierarchical variable</u>				
7	Nominal	Random	Flight Number	Identification number of flight

212
 213 Continuous variables were group-centred. Two separate base data models were created for the TIR
 214 images and RGB images. In the TIR base data model, the variable colour was not included since the
 215 TIR images only display in black and white. The inclusion of Flight Number as a random intercept
 216 significantly improved the TIR data model. However, random effects did not improve the RGB base
 217 data model and so a general linear model was used (using the “glm” function in the “glm2”
 218 package: Marschner, 2018). Maximum likelihood was used to perform the model estimation for
 219 both data models. Data sub-models were created from the base data models, using the function
 220 “dredge” from the “MuMIn” (Bartón, 2017) packages as described by Grueber et al. (2011). This
 221 resulted in a total of 64 data sub-models for the RGB images and 32 data sub-models for the TIR
 222 images. The Akaike Information Criterion corrected for small sample sizes (AICc) was used to

223 assess the data (sub) models (Akaike, 1998; Grueber et al., 2011). Data models with cut-off values
224 of 2AICc were selected using the “get.model” function from the “MuMIn” packages as shown by
225 (Bartón, 2016; Grueber et al., 2011). The final data models above this cut-off point were averaged
226 using the zero method to compare between them and identify the one with the best fit (Nakagawa
227 and Freckleton, 2011). These data models have been ranked by their AICc values and their Akaike
228 weight (lower AICc indicates a better model fit and a higher Akaike weight shows a more
229 parsimonious fit overall) (Patterson et al., 2016). The last step was to conduct a Tukey’s honestly
230 significant difference (HSD) analysis with the “glht” function from the “multcomp” package
231 (Hothorn et al., 2008; Piepho, 2004) to analyse the differences between individual colours and their
232 effect on the probability of detection.

233

234 **3 Results**

235 To determine which factors influenced detection probability we fitted models to the TIR and RGB
 236 data. The analyses are first presented individually and then compared.

237

238 **3.1. TIR data model**

239 For the TIR data model, three models were selected under the described AICc criterion (Table 2).

240 *Canopy density, Distance and Analyst* were included in the best data model.

241 *Table 2: A summary of the three selected data models under the AICc criterion (from 32 data sub*
 242 *models) for the detection of subjects using a TIR imaging camera. The best data model includes*
 243 *Canopy density, Distance and Analyst.*

Data model name	Df	LogLik	AICc	Delta	weight
Canopy density + Distance + Analyst	5	-1117.35	2244.72	0.00	0.50
Canopy density + Distance + Time of Day + Analyst	6	-1116.84	2245.72	1.00	0.31
Canopy density + Time of Day + Altitude + Analyst	6	-1117.31	2246.66	1.94	0.19

244

245 For the TIR data model, three data models were selected under the described criterion (Table 2).

246 The best data model contained the variables *Canopy density, Distance and Analyst*. The best fitting
 247 data model is described in Table 3 in more detail.

248 *Table 3: The data model with the best fit for the TIR images include the variables Canopy density*
 249 *($p < 0.001$), Distance ($p < 0.001$) and Analyst ($p = 0.005$).*

Variable	Estimate	95% Confident	Standard Error	p
(Intercept)	0.082202	-0.57588189, 0.74028561	0.335592	0.807
Canopy density	-2.512167	-2.93676277, -2.08757128	0.216496	<0.001
Distance	-0.040112	-0.04966423, -0.03056052	0.004870	<0.001
Analyst	-0.178310	-0.30211515, -0.05450457	0.063127	0.005

250

251 The variables *Canopy density* and *Distance* had negative coefficients, which indicates a decrease in
 252 the probability of detection with an increase in vegetation density and/or increase in distance from
 253 the centreline. The negative coefficient for *Analyst* is irrelevant since analysts were ranked in a
 254 random order.

255

256 **3.2. RGB data model**

257 The best data model for the RGB data included *Canopy density*, *Altitude*, *Colour*, and *Analyst* as
 258 variables (Table 4). All of these variables were significant (Table 5). The variables *Canopy density*
 259 and *Altitude* had negative coefficients, which indicates that an increase in the vegetation density and
 260 altitude negatively influences the probability of detection. The variable *Colour* also had a
 261 significant effect on the probability of detection while the variable *Distance* was not included in the
 262 best data model, which indicates it does not affect the probability of detection. As in the TIR model,
 263 the negative coefficient for *Analyst* was meaningless.

265 *Table 4: A summary of the top three data models that were selected under the 2AICc criteria (from*
 266 *64 data sub-models) for the RGB camera. Canopy density, Altitude, Colour and Analyst are*
 267 *included in the best data model.*

Data model name	Df	LogLik	AICc	Delta	weight
Canopy density + Altitude + Colour + Analyst	5	-352.23	714.53	0.00	0.54
Canopy density + Altitude + Colour + Time of Day + Analyst	6	-352.02	716.15	1.62	0.24
Canopy density + Distance + Altitude + Colour + Analyst	6	-352.10	716.31	1.78	0.22

268

269 *Table 5: The best fitting RGB data model includes Canopy density ($p < 0.001$), Altitude ($p < 0.001$),*
 270 *Colour ($p = 0.012$) and Analyst ($p = 0.013$).*

Variable	Estimate	95% Confident	Standard Error	p
(Intercept)	0.0697321	-0.60499062, 0.74445474	0.3437274	0.840
Canopy density	-4.4783526	-5.33703130, -3.61967387	0.4374412	<0.001
Altitude	-0.9168489	-1.29410419, -0.53959361	0.1921870	<0.001
Colour	-0.3111846	-0.55472733, -0.06764184	0.1240692	0.012
Analyst	-0.2884761	-0.51514749, -0.06180480	0.1154742	0.013

271

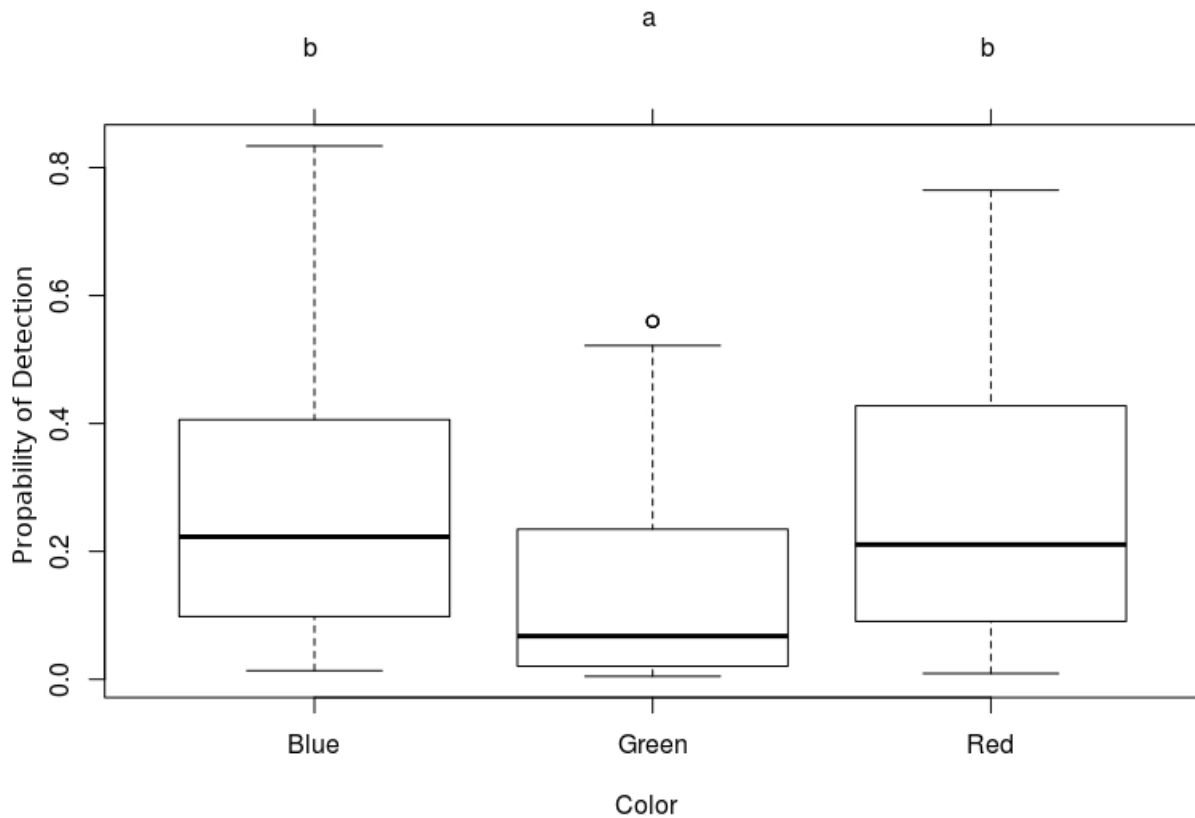


Figure 1. Box-and-whisker plots that summarize detection probabilities for the three t-shirt colours worn by subjects.

272 All variables included in the best fitting RGB data model have a negative coefficient indicating that
 273 an increase in *Canopy density* and *Altitude* have a negative effect on the probability of detection.
 274 The *Colour* variable was further analysed with a Tukey’s HSD post-hoc test to assess which colours
 275 were significantly different (Figure 1). The Tukey’s HSD analysis showed that the probability of
 276 detection of a green subject (a) was significantly lower than the probability of detection of either a
 277 blue or red t-shirt (b) (Figure 1).

278

279 3.3. Comparison

280 The overall detection probability was higher
 281 for TIR images than for RGB images (Figure
 282 2). A two sample t-test showed a significant
 283 ($p < 0.005$) difference in mean detection
 284 probabilities between RGB and TIR images.
 285 The best fitting models were compared for
 286 TIR and RGB images. Only *Canopy density*

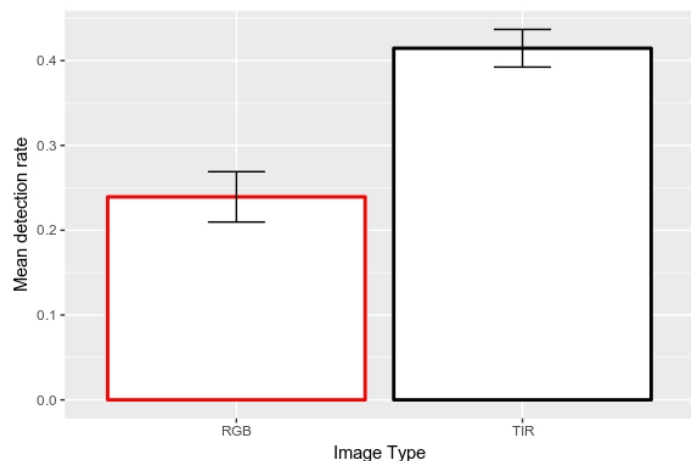


Figure 2. Bar charts that summarize mean subject detection probability with standard error.

287 (negative coefficient) and *Analyst* were included in both data models. *Distance* was only included in
288 the TIR data model, whereas *Altitude* and *Colour* were included in the RGB data model. As
289 previously stated, *Colour* was not included in the TIR base data model.
290 It is important to note that *Time of Day* was not significant in either data model.

291 **4 Discussion**

292 We aimed to identify factors that have a significant effect on the probability of detection of
293 poachers by drones using two camera types (RGB and TIR). Factors that had a significant effect on
294 the probability of detection by TIR images were canopy density, subject distance from the image
295 centreline and the image analyst, while the RGB camera was significantly affected by canopy density,
296 altitude of the drone, the subjects' contrast against the background and the image analyst.

297 Canopy density had a significant negative influence on detection probability for both cameras. This
298 is in accordance with studies on aerial surveying of animals that have found that vegetation density
299 or habitat type has a significant negative impact on probability of detection (Chrétien et al., 2015;
300 Ransom, 2012; Schlossberg et al., 2016; Zabransky et al., 2016). Our results are also consistent with
301 a study that found that habitat type had a significant impact on detection of caribou (Patterson et al.
302 2016).

303 Our study also showed a decrease in detection probability with increasing distance from the image
304 centreline, for TIR images. In contrast, no equivalent effect was found in our RGB analysis or by a
305 previous caribou study (Patterson et al., 2016). The latter used a 50-mm lens on a full-frame camera
306 attached to the drone resulting in a FOV of 40°. On this system, distortion and other effects towards
307 the edges of the frame are minimal and it could thus be expected that no effect would be observed.
308 Our RGB camera had a wide-angle lens with a FOV of 82° and therefore has a greater distortion
309 than a normal lens (Brauer-Burchardt and Voss, 2001). In contrast, the TIR camera we deployed in
310 our study had a narrow FOV of 45°. This runs counter to the suggestion that greater distortion from
311 a wider FOV could explain the significant effect for the TIR but not the RGB camera. We were
312 unable to find any similar reports in literature, however, the impact of the distance from the
313 centreline on the probability of detection is well-known in line-transect surveys (Ridgway, 2010).
314 Other studies have hypothesized that subjects' distance from the centreline is affected by the height
315 of the canopy (Israel, 2011).

316 The RGB images revealed that detection was strongly influenced by the subjects' colour against the
317 background. A similar effect was found by Patterson et al. (2016) who found that targets with
318 greater contrast against the landscape were more easily detected. Detection is also impeded by
319 greater contrast variation in the image background, as this results in variable contrast of the subject
320 against the background (Abd-Elrahman et al., 2005). Chrétien et al. (2015) found animals with
321 cryptic fur have a lower probability of detection because they blend into their environment. Hence,
322 our findings add to previous studies that have shown that aspects of colour, such as contrast, affect
323 the probability detection using RGB images.

324 Higher flight altitudes also showed lower detection probabilities for RGB images. One way around
325 this might be to use the full resolution original images. Patterson et al. (2016) flew at a constant
326 altitude of around 690 m with no significant variation in elevation in the study area; and therefore
327 was not able to test for the effect of altitude on the probability of detection. However, our results do
328 suggest that the TIR imaging camera is superior at higher flight elevations for the same number of
329 pixels. This could be important in cases where drones must be flown low or where drone height
330 above ground will vary considerably over an area being investigated.

331 Another significant effect in the data models was the variation in detection probabilities between
332 observers. Patterson et al. (2016) did not find an analyst effect in their study. A possible explanation
333 might be that Patterson et al. (2016) used a controlled procedure for the analysts who were
334 instructed to work through a fixed number of images per day, while the analysts themselves had no
335 previous experience. In our study the analyst effect might be due to the use of three different
336 analysts, with different experience levels.

337 Time of day was included as factors in the present study for RGB and TIR images, however no
338 significant difference was found. In contrast, Patterson et al. (2016) found a significant time of day
339 effect. Nonetheless, their flights were performed in a larger time window (7:00 – 9:30 am and 2:00
340 – 3:00 pm), with more targets being detected in the afternoon. Also, their study site was in
341 Labrador, Canada with potentially very different changes in light level between the two flight
342 periods, relative to Tanzania.

343 An increasing number of research projects are examining the use of drones for ecological
344 conservation and anti-poaching efforts (Chrétien et al., 2015; Christiansen et al., 2014; Christie et
345 al., 2016; Linchant et al., 2015; Martin et al., 2012; Mukwazvure and Magadza, 2014; Mulero-
346 Pázmány et al., 2014; Olivares-Mendez et al., 2015; Patterson et al., 2015; Vermeulen et al., 2013).
347 This is the first study to focus on poacher-detection and the first to explore the factors affecting
348 detection probabilities for TIR imaging. Most other studies that have examined TIR imaging with
349 drones have focused on the automated detection of animals and humans, which is essential to
350 reduce the researcher-hours spent on analysing images and can facilitate near-real time detection of
351 animals/humans in the field (Christiansen et al., 2014; Gonzalez et al., 2016; Longmore et al., 2017;
352 McMillen, 2016; Olivares-Mendez et al., 2015; Seymour et al., 2017). Burke et al. (2018b) applied
353 automatic detection software to the TIR images used in our study. Promising methods for increased
354 detection probabilities lie in the integration of data from multiple sensors such as RGB and TIR
355 cameras (Chrétien et al., 2015; Christiansen et al., 2014).

356 In conclusion, the TIR images allowed for higher detection probability of our experimental
357 poachers than RGB images. This provides a clear advantage against poachers are trying to hide

358 under vegetation, wear low-contrast clothing, or operate at night. However, during the daytime,
359 when temperatures are higher, the RGB performs better than the TIR camera. As expected,
360 poachers hiding under thick vegetation remain undetected with both systems. Distance from the
361 flight midline also influenced detection and should be considered when conducting anti-poaching
362 missions. Potential improvements to detect poachers under trees might be achieved by use of a
363 camera placed at an oblique angle as well as use of machine learning for detection instead of human
364 image analysts.

365

366 **5 Glossary**

367 **Altitude:** The altitude of the drone measured from the take-off point.

368 **Analyst:** Person who reviewed each image from the drone and marks every person detected in the
369 images.

370 **Canopy Cover:** Percentage of canopy covering the location compared to open sky.

371 **Colour:** Test subject have been wearing uniform red, green or blue coloured t-shirt to create a
372 controlled contrast against the green vegetation in the background.

373 **Distance:** The distance of a test subject to the centreline of an image in meters.

374 **Field of View (FOV):** A measurement of a lens in degrees of the area in front of the lens which is
375 been captured.

376 **Probability of Detection:** The likelihood that an object is been detecting.

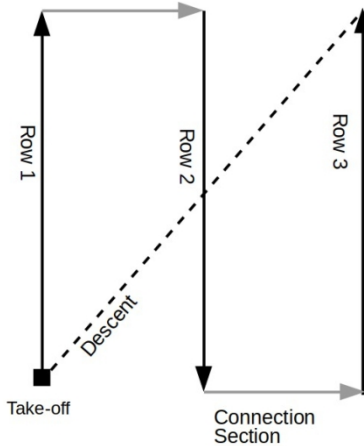
377 **Red Green Blue (RGB):** Colour model used by most common cameras today.

378 **Time of Day:** Variable to compare the influence of dawn and dusk on the probability of detection.

379 **Thermal Infrared (TIR):** A wave spectrum which is radiated by warm objects.

380 **6 Appendix**

381 **A. Flight pattern**

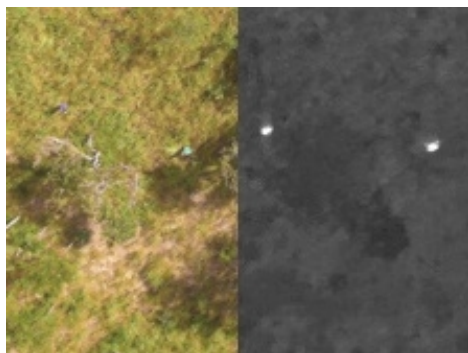


Appendix A: Flight pattern of the drone. Each row is 70 m in length and the Connection Sections are 30 m long. The Decent leads the drone back to the Take-off area.

382

383

384 **B. Comparison between RGB and TIR images.**



Appendix B: Comparison between RGB images on the left and TIR on right. Both images show the same area, at the same resolution with two people visible.

385
386

387 Appendix B to be printed in colour

388 **References**

- 389 Abd-Elrahman, A., Pearlstine, L., Percival, F., 2005. Development of pattern recognition algorithm
390 for automatic bird detection from unmanned aerial vehicle imagery. *Surv. Land Inf. Sci.* 65,
391 37.
- 392 Air Shepherd, 2017. Home - Air Shepherd [WWW Document]. URL <http://airshepherd.org/>
393 (accessed 4.6.17).
- 394 Akaike, H., 1998. Information theory and an extension of the maximum likelihood principle, in:
395 Selected Papers of Hirotugu Akaike. Springer, pp. 199–213.
- 396 ArduPilot Dev Team, 2017. Mission Planner. ArduPilot.
- 397 Baggaley, K., 2017. Drones are setting their sights on wildlife | Popular Science [WWW
398 Document]. URL <http://www.popsci.com/drones-wildlife-biology-animal-research> (accessed
399 8.24.17).
- 400 Balazs, E., 2016. From Poaching to Financing Terrorism: Thoughts on Poaching Endangering
401 Society. *JE-Eur Crim L* 190.
- 402 Bartón, K., 2017. Multi-model inference. R package version 1.40.0. 2017.
- 403 Bates, D., Maechler, M., Bolker, B., Walker, S., Christensen, R.H.B., Singmann, H., Dai, B.,
404 Grothendieck, G., Green, P., 2017. lme4: Linear Mixed-Effects Models using “Eigen” and
405 S4.
- 406 Becker, M., McRobb, R., Watson, F., Droge, E., Kanyembo, B., Murdoch, J., Kakumbi, C., 2013.
407 Evaluating wire-snare poaching trends and the impacts of by-catch on elephants and large
408 carnivores. *Biol. Conserv.* 158, 26–36.
- 409 Brauer-Burchardt, C., Voss, K., 2001. A new algorithm to correct fish-eye-and strong wide-angle-
410 lens-distortion from single images, in: *Image Processing, 2001. Proceedings. 2001*
411 *International Conference On. IEEE*, pp. 225–228.
- 412 Burke, C., Rashman, M., Wich, S., Symons, A., Theron, C., Longmore, S., 2018a. Optimising
413 observing strategies for monitoring warm-blooded animal species using UAV-mounted
414 thermal infrared cameras. - *Ternational J. Remote Sens.* in press.
- 415 Burke, C., Rashman, M.R., McAgree, O., Hambrecht, L., Longmore, S.N., Piel, A.K., Wich, S.A.,
416 2018b. Addressing environmental and atmospheric challenges for capturing high-precision
417 thermal infrared data in the field of astro-ecology, in: *Astronomical Telescopes +*
418 *Instrumentation*. Presented at the SPIE, Austin, Texas, US. In press.
- 419 Caughley, G., Sinclair, R., Scott-Kemmis, D., 1976. Experiments in aerial survey. *J. Wildl. Manag.*
420 290–300.
- 421 Chapron, G., Miquelle, D.G., Lambert, A., Goodrich, J.M., Legendre, S., Clobert, J., 2008. The
422 impact on tigers of poaching versus prey depletion. *J. Appl. Ecol.* 45, 1667–1674.
- 423 Chrétien, L.P., Théau, J., Ménard, P., 2015. Wildlife multispecies remote sensing using visible and
424 thermal infrared imagery acquired from an unmanned aerial vehicle (UAV). *Int. Arch.*
425 *Photogramm. Remote Sens. Spat. Inf. Sci.* 40, 241.
- 426 Chrétien, L.P., Théau, J., Ménard, P., 2016. Visible and thermal infrared remote sensing for the
427 detection of white-tailed deer using an unmanned aerial system. *Wildlife Society Bulletin*
428 40, 181–191.
- 429 Christiansen, P., Steen, K.A., Jørgensen, R.N., Karstoft, H., 2014. Automated detection and
430 recognition of wildlife using thermal cameras. *Sensors* 14, 13778–13793.
- 431 Christie, K.S., Gilbert, S.L., Brown, C.L., Hatfield, M., Hanson, L., 2016. Unmanned aircraft
432 systems in wildlife research: current and future applications of a transformative technology.
433 *Front. Ecol. Environ.* 14, 241–251.
- 434 De Vos, K., 2010. Cell counter plugin for ImageJ.
- 435 Dinerstein, E., Olson, D., Joshi, A., Vynne, C., Burgess, N.D., Wikramanayake, E., Hahn, N.,
436 Palminteri, S., Hedao, P., Noss, R., Hansen, M., Locke, H., Ellis, E.C., Jones, B., Barber,
437 C.V., Hayes, R., Kormos, C., Martin, V., Crist, E., Sechrest, W., Price, L., Baillie, J.E.M.,
438 Weeden, D., Suckling, K., Davis, C., Sizer, N., Moore, R., Thau, D., Birch, T., Potapov, P.,
439 Turubanova, S., Tyukavina, A., de Souza, N., Pintea, L., Brito, J.C., Llewellyn, O.A.,

440 Miller, A.G., Patzelt, A., Ghazanfar, S.A., Timberlake, J., Klöser, H., Shennan-Farpon, Y.,
441 Kindt, R., Lillesø, J.-P.B., van Breugel, P., Graudal, L., Voge, M., Al-Shammari, K.F.,
442 Saleem, M., 2017. An Ecoregion-Based Approach to Protecting Half the Terrestrial Realm.
443 *BioScience* 67, 534–545. <https://doi.org/10.1093/biosci/bix014>
444 Field, A.P., Miles, J., Field, Z., 2012. Multilevel linear models, in: *Discovering Statistics Using R*.
445 Sage publications, London; Thousand Oaks, Calif, pp. 855–909.
446 Gonzalez, L.F., Montes, G.A., Puig, E., Johnson, S., Mengersen, K., Gaston, K.J., 2016. Unmanned
447 Aerial Vehicles (UAVs) and artificial intelligence revolutionizing wildlife monitoring and
448 conservation. *Sensors* 16, 97.
449 Goodenough, A.E., Goodenough, A.S., 2012. Development of a rapid and precise method of digital
450 image analysis to quantify canopy density and structural complexity. *ISRN Ecol.* 2012.
451 Goodenough, Anne, Goodenough, Andrew, 2016. *CanopyDigi*.
452 Grueber, C.E., Nakagawa, S., Laws, R.J., Jamieson, I.G., 2011. Multimodel inference in ecology
453 and evolution: challenges and solutions: Multimodel inference. *J. Evol. Biol.* 24, 699–711.
454 <https://doi.org/10.1111/j.1420-9101.2010.02210.x>
455 Harvey, P., 2017. ExifTool: Read, write and edit meta information. *Softw. Package Available*
456 <https://www.sno.phy.queensu.ca/~phil/exiftool/>.
457 Hodgson, J.C., Mott, R., Baylis, S.M., Pham, T.T., Wotherspoon, S., Kilpatrick, A.D., Raja
458 Segaran, R., Reid, I., Terauds, A., Koh, L.P., 2018. Drones count wildlife more accurately
459 and precisely than humans. *Methods Ecol. Evol.* 9, 1160–1167.
460 Hothorn, T., Bretz, F., Westfall, P., 2008. Simultaneous inference in general parametric models.
461 *Biom. J.* 50, 346–363.
462 Israel, M., 2011. A UAV-based roe deer fawn detection system. *Int. Arch. Photogramm. Remote*
463 *Sens.* 38, 1–5.
464 Kakaes, K., Greenwood, F., Lippincott, M., Dosemagen, S., Meier, P. and Wich, S., 2015. Drones
465 and aerial observation: New technologies for property rights, human rights, and global
466 development. *New America*, Washington, DC, USA, Tech. Rep.
467 Koh, L.P., Wich, S.A., 2012. Dawn of drone ecology: low-cost autonomous aerial vehicles for
468 conservation. *Trop. Conserv. Sci.* 5, 121–132.
469 Lawson, K., Vines, A., 2014. *Global impacts of the illegal wildlife trade: The costs of crime,*
470 *insecurity and institutional erosion.* Chatham house.
471 Liberg, O., Chapron, G., Wabakken, P., Pedersen, H.C., Hobbs, N.T., Sand, H., 2012. Shoot, shovel
472 and shut up: cryptic poaching slows restoration of a large carnivore in Europe. *Proc R Soc B*
473 279, 910–915.
474 Linchant, J., Lisein, J., Semeki, J., Lejeune, P., Vermeulen, C., 2015. Are unmanned aircraft
475 systems (UASs) the future of wildlife monitoring? A review of accomplishments and
476 challenges. *Mammal Rev.* 45, 239–252.
477 Longmore, S.N., Collins, R.P., Pfeifer, S., Fox, S.E., Mulero-Pázmány, M., Bezombes, F.,
478 Goodwin, A., De Juan Ovelar, M., Knapen, J.H., Wich, S.A., 2017. Adapting astronomical
479 source detection software to help detect animals in thermal images obtained by unmanned
480 aerial systems. *Int. J. Remote Sens.* 38, 2623–2638.
481 Lunstrum, E., 2014. Green militarization: anti-poaching efforts and the spatial contours of Kruger
482 National Park. *Ann. Assoc. Am. Geogr.* 104, 816–832.
483 Mapir, C., 2016a. Survey2 Cameras [WWW Document]. *MAPIR CAMERA*. URL
484 <https://www.mapir.camera/collections/survey2> (accessed 5.29.18).
485 Mapir, C., 2016b. Pre-Process Survey2 Images in Fiji with MAPIR Plugin.
486 Marschner, I., 2018. *glm2: Fitting Generalized Linear Models*.
487 Martin, J., Edwards, H.H., Burgess, M.A., Percival, H.F., Fagan, D.E., Gardner, B.E., Ortega-Ortiz,
488 J.G., Ifju, P.G., Evers, B.S., Rambo, T.J., 2012. Estimating distribution of hidden objects
489 with drones: From tennis balls to manatees. *PLoS One* 7, e38882.
490 McMillen, D., 2016. Investigating limitations of SURF approach for thermal imaging analysis and
491 mapping.

492 Mukwazvure, A., Magadza, T.B., 2014. A survey on anti-poaching strategies. Unspecified 3.

493 Mulero-Pázmány, M., Stolper, R., Van Essen, L.D., Negro, J.J., Sassen, T., 2014. Remotely piloted
494 aircraft systems as a rhinoceros anti-poaching tool in Africa. *PloS One* 9, e83873.

495 Naidoo, R., Fisher, B., Manica, A., Balmford, A., 2016. Estimating economic losses to tourism in
496 Africa from the illegal killing of elephants. *Nat. Commun.* 7, 13379.
497 <https://doi.org/10.1038/ncomms13379>

498 Nakagawa, S., Freckleton, R.P., 2011. Model averaging, missing data and multiple imputation: a
499 case study for behavioural ecology. *Behav. Ecol. Sociobiol.* 65, 103–116.

500 Olivares-Mendez, M.A., Fu, C., Ludivig, P., Bissyandé, T.F., Kannan, S., Zurad, M., Annaiyan, A.,
501 Voos, H., Campoy, P., 2015. Towards an autonomous vision-based unmanned aerial system
502 against wildlife poachers. *Sensors* 15, 31362–31391.

503 Parveen, N., 2016. British pilot in Tanzania “manoeuvred to save colleague before death.” *The*
504 *Guardian*.

505 Patterson, C., Koski, W., Pace, P., McLuckie, B., Bird, D.M., 2015. Evaluation of an unmanned
506 aircraft system for detecting surrogate caribou targets in Labrador. *J. Unmanned Veh. Syst.*
507 4, 53–69.

508 Piel, A.K., Lenoel, A., Johnson, C., Stewart, F.A., 2015. Detering poaching in western Tanzania:
509 the presence of wildlife researchers. *Glob. Ecol. Conserv.* 3, 188–199.

510 Piepho, H.-P., 2004. An algorithm for a letter-based representation of all-pairwise comparisons. *J.*
511 *Comput. Graph. Stat.* 13, 456–466.

512 Qian, S.S., Cuffney, T.F., Alameddine, I., McMahon, G., Reckhow, K.H., 2010. On the application
513 of multilevel modeling in environmental and ecological studies. *Ecology* 91, 355–361.

514 Quantum GIS Development Team, 2017. Quantum GIS Geographic Information System. Open
515 Source Geospatial Foundation Project.

516 R Core Team, 2017. R: A language and environment for statistical computing. R Foundation for
517 Statistical Computing, Vienna, Austria.

518 Ransom, J.I., 2012. Detection probability in aerial surveys of feral horses. *J. Wildl. Manag.* 76,
519 299–307.

520 ReaSoft Development, 2017. reaConverter - Batch image converter that makes it easy to work on
521 millions of files and folders in a single operation.

522 Ridgway, M.S., 2010. Line transect distance sampling in aerial surveys for double-crested
523 cormorants in coastal regions of Lake Huron. *J. Gt. Lakes Res.* 36, 403–410.

524 Rueden, C.T., Schindelin, J., Hiner, M.C., DeZonia, B.E., Walter, A.E., Arena, E.T., Eliceiri, K.W.,
525 2017. ImageJ2: ImageJ for the next generation of scientific image data. *BMC*
526 *Bioinformatics* 18, 529.

527 Schindelin, J., Arganda-Carreras, I., Frise, E., Kaynig, V., Longair, M., Pietzsch, T., Preibisch, S.,
528 Rueden, C., Saalfeld, S., Schmid, B., 2012. Fiji: an open-source platform for biological-
529 image analysis. *Nat. Methods* 9, 676.

530 Schlossberg, S., Chase, M.J., Griffin, C.R., 2016. Testing the accuracy of aerial surveys for large
531 mammals: an experiment with African savanna elephants (*Loxodonta africana*). *PloS One*
532 11, e0164904.

533 Seymour, A.C., Dale, J., Hammill, M., Halpin, P.N., Johnston, D.W., 2017. Automated detection
534 and enumeration of marine wildlife using unmanned aircraft systems (UAS) and thermal
535 imagery. *Sci. Rep.* 7, 45127.

536 Smart parks, 2018. Track record SmartParks [WWW Document]. Smartparks Found. URL
537 <https://www.smartparks.org/track-record/> (accessed 5.25.18).

538 Tanzania Civil Aviation Authority, 2017. AIC 5/17 (pink 62) 1 JAN 2017 - Unmanned Aircraft
539 Systems, 5/17.

540 TeAx Technology, 2017. ThermoViewer | ThermalCapture - Thermal Imaging Technology.

541 TeAx Technology, 2018. Flir Tau 2 640 [WWW Document]. URL <http://thermalcapture.com/flir-tau-2-640/> (accessed 5.12.18).

542

543 Trimble Navigation Limited, Trimble, 2013. MobileMapper 20 - Getting Started Guide.

544 United Nations Office on Drugs and Crime, 2016. World wildlife crime report: trafficking in
545 protected species, 2016, United Nations publication. United Nations, New York.
546 Vermeulen, C., Lejeune, P., Lisein, J., Sawadogo, P., Bouché, P., 2013. Unmanned aerial survey of
547 elephants. *PLoS One* 8, e54700.
548 Vollmer, M., Möllmann, K.-P., 2010. Infrared thermal imaging: fundamentals, research and
549 applications. John Wiley & Sons.
550 Wich, S.A., Koh, L.P., 2018. Conservation Drones: Mapping and Monitoring Biodiversity. Oxford
551 University Press.
552 World Bank, 2018. Tools and Resources to Combat Illegal Wildlife Trade.
553 Wride, M.C., Baker, K., 1977. Thermal imagery for census of ungulates. NASA.
554 Zabransky, C.J., Hewitt, D.G., Deyoung, R.W., Gray, S.S., Richardson, C., Litt, A.R., Deyoung,
555 C.A., 2016. A detection probability model for aerial surveys of mule deer. *J. Wildl. Manag.*
556 80, 1379–1389.
557